J|A|C|S ARTICLES

Published on Web 10/15/2010

Influence of Concentration and Temperature on the Dynamics of Water in the Hydrophobic Hydration Shell of Tetramethylurea

Klaas-Jan Tielrooij,[†] Johannes Hunger,[†] Richard Buchner,[‡] Mischa Bonn,[†] and Huib J. Bakker*,[†]

FOM Institute Amolf, Science Park 104 1098 XG Amsterdam, The Netherlands, and Institute of Physical and Theoretical Chemistry, University of Regensburg, 93040 Regensburg, Germany

Received July 15, 2010; E-mail: bakker@amolf.nl

Abstract: We study the influence of the amphipilic compound tetramethylurea (TMU) on the dynamical properties of water, using dielectric relaxation spectroscopy in the regime between 0.2 GHz and 2 THz. This technique is capable of resolving different water species, their relative fractions, and their corresponding reorientation dynamics. We find that the reorientation dynamics of water molecules in the hydration shell of the hydrophobic groups of TMU is between 3 (at low concentrations) and 10 (at higher concentrations) times slower than the dynamics of bulk water. The data indicate that the effect of hydrophobic groups on water is strong but relatively short-ranged. With increasing temperature, the fraction of water contained in the hydrophobic hydration shell decreases, which implies that the overall effect of hydrophobic groups on water becomes smaller.

Introduction

The interaction between hydrophobes and water is of fundamental chemical interest, and is highly relevant for biochemistry and biology. Molecules that are essential in biology, such as proteins, change the structure and dynamics of the surrounding water shell, whereas this water hydration layer, in turn, affects the functioning of these biomolecules.[1] In hydrophobic interactions, a distinction is generally made between small and large hydrophobes. For the former (length <1 nm), water molecules can adopt orientations that allow the hydrogen-bond network to go around the solute, whereas in the latter case (length >1 nm), the extended solute surface makes it impossible for adjacent water molecules to maintain a complete hydrogen-bonding network with the surrounding liquid.[2] The hydration of (small) hydrophobes has been studied using numerous techniques. Besides theoretical work,[2−5] it has been a popular subject for experimental investigations. Earlier studies examined mainly thermodynamic properties[6] and found that upon mixing hydrophobes and water, the system experiences negative changes in enthalpy and excess entropy. Later studies examined structural and dynamical properties on a molecular level.[7−20]

The various measurements and computer simulations have so far led to some consistent and some contradictory conclusions. The negative changes in enthalpy and excess entropy from ref 6 were originally thought to be caused by an enhancement in the structure of the water network around the hydrophobic solute. This enhancement was, however, not observed in neutron diffraction measurements that probe the structural properties of aqueous solutions of hydrophobic molecules.[7,8] New insights were gained by NMR, dielectric relaxation (DR), and femtosecond infrared pump−probe (fs-IR) studies of the reorientation dynamics of water molecules hydrating hydrophobes. These studies showed that it is not the structure of water that is affected by the presence of the hydrophobe, but rather the reorientational dynamics: water in the hydrophobic hydration shell was found to be slowed in its rotational motion.[9−18] From these DR and fs-IR studies, it was concluded that a strong retardation occurs

[†] FOM Institute Amolf.
[‡] University of Regensburg.

(1) Ball, P. *Chem. Rev.* **2008**, *108*, 74–108.
(2) Chandler, D. *Nature* **2005**, *437*, 640–647.
(3) Laage, D.; Stirnemann, G.; Hynes, J. T. *J. Phys. Chem. B* **2009**, *113*, 2428–2435.
(4) Wei, H.; Fan, Y.; Gao, Y. Q. *J. Phys. Chem. B* **2010**, *114*, 557–568.
(5) Silvestrelli, P. L. *J. Phys.Chem. B* **2009**, *113*, 10728–10731.
(6) Frank, H. S.; Evans, M. W. *J. Chem. Phys.* **1945**, *13*, 507–532.
(7) Soper, A. K.; Finney, J. L. *Phys. Rev. Lett.* **1993**, *71*, 4346–4349.
(8) Blokzijl, W.; Engberts, J. B. F. N. *Angew. Chem., Int. Ed. Engl.* **1993**, *32*, 1545–1579.
(9) Ishihara, Y.; Okouchi, S.; Uedaira, H. *J. Chem. Soc., Faraday Trans.* **1997**, *93*, 3337–3342.
(10) Shimizu, A.; Fumino, K.; Yukiyasu, K.; Taniguchi, Y. *J. Mol. Liq.* **2000**, *85*, 269–278.
(11) Fumino, K.; Yukiyasu, K.; Shimizu, A.; Taniguchi, Y. *J. Mol. Liq.* **1998**, *75*, 1–12.
(12) Yoshida, K.; Ibuki, K.; Ueno, M. *J. Chem. Phys.* **1998**, *108*, 1360–1367.
(13) Qvist, J.; Halle, B. *J. Am. Chem. Soc.* **2008**, *130*, 10345–10353.
(14) Kaatze, U.; Rupprecht, A. *J. Chem. Phys.* **2002**, *117*, 4936–4939.
(15) Hallenga, K.; Grigera, J. R.; Berendsen, H. J. C. *J. Phys. Chem.* **1980**, *84*, 2381–2390.
(16) Buchner, R.; Hölzl, C.; Stauber, J.; Barthel, J. *Phys. Chem. Chem. Phys.* **2002**, *4*, 2169–2179.
(17) Rezus, Y. L. A.; Bakker, H. J. *J. Phys. Chem. A* **2008**, *112*, 2355–2361.
(18) Rezus, Y. L. A.; Bakker, H. J. *Phys. Rev. Lett.* **2007**, *99*, 148301.
(19) Bakulin, A. A.; Liang, C.; la Cour Jansen, T.; Wiersma, D. W.; Bakker, H. J.; Pshenichnikov, M. S. *Acc. Chem. Res.* **2009**, *42*, 1229–1238.
(20) Petersen, C.; Tielrooij, K. J.; Bakker, H. J. *J. Chem. Phys.* **2009**, *130*, 214511.

of the rotational dynamics of a limited number of water molecules hydrating the hydrophobic group. These results are consistent with NMR measurements,[9−13] from which the average reorientation time of all water molecules can be obtained. As a result, in NMR the size of the hydration shell needs to be assumed to infer the degree of retardation of the hydration shell water. Fs-IR measurements do not have this disadvantage, because the full orientational correlation function is measured. However, fs-IR measurements have the disadvantage that the time window is restricted to about 10 ps, which limits the possibility of extracting time scales that are much outside this window. Hence, these measurements unfortunately cannot quantify the time scale of the slowed reorientation, nor determine precisely how many water molecules are slowed, or why they are slowed.

Classical molecular dynamics simulations have shown a relatively modest retardation effect for amphiphilic molecules, which was assigned to be a purely geometric effect: the excluded volume that is occupied by the solute[3] prevents a water molecule in the hydration shell from being approached by another water molecule to which it would hydrogen-bond after the reorientation process. These simulations furthermore suggested that for most solutes the major effect in the hydration dynamics comes from the hydrophilic group,[21] which does not agree with the observation that the effect on the water dynamics scales with the size of the hydrophobic part, as found by NMR[10,13] and fs-IR.[18]

The key in solving these apparent controversies is being able to resolve simultaneously, and in a model-independent way, the different water species, their relative fractions, and their corresponding reorientation dynamics. To this end, we combine in this study two complementary dynamical techniques, to reach a better molecular level understanding of hydrophobic hydration of the prototypical hydrophobe tetramethylurea (TMU). GHz−THz DR measurements over four decades in frequency space were performed for TMU:water mixtures over a wide range of concentrations, and the results are compared to literature data from fs-IR, as measured by Rezus et al.[17] GHz−THz DR measurements were also performed for a TMU:water mixture at different temperatures to get more clarity on whether the number of hydration shell water molecules with slowed reorientation dynamics depends on temperature.

Experimental Section

Dielectric relaxation measurements probe the macroscopic polarization of a sample as a function of frequency, which in the case of an uncharged polar liquid reflects the reorientation of dipoles. If an oscillating electromagnetic field is impinging on a polar liquid, the permanent dipoles of the polar molecules try to align with the oscillating electric field. When the frequency of the oscillations is too high, the dipoles cannot keep up reorienting with the field and start lagging behind, leading to marked changes in the dielectric properties of the sample. It is thus possible to measure dielectric spectra, where the complex permittivity of a sample is measured as a function of frequency of the electromagnetic probing field. The complex dielectric function or permittivity $\hat{\varepsilon} = \varepsilon' - i\varepsilon'' = (n - ik)^2$ contains information about refraction (n is the refractive index) and absorption (k is the extinction coefficient). For a typical polar liquid with a single dielectric relaxation process, ε depends on the angular frequency ω according to

$$\varepsilon(\omega) = \frac{\varepsilon_S - \varepsilon_\infty}{1 + i\omega\tau} + \varepsilon_\infty \quad (1)$$

where ε_S and ε_∞ are the zero and infinite frequency limits, respectively; and τ is the relaxation time. The in-phase part of the dielectric function ε' in eq 1 shows a smooth decrease from ε_S to ε_∞, whereas the out-of-phase response (ε'' or dielectric loss) shows a peak in absorption at an angular frequency $1/\tau$. The macroscopic relaxation time τ is directly related to the reorientation time of dipolar species in the sample. By combining electrical sources and optical sources, a large range of probing frequencies (200 MHz − 2 THz) is covered, making this technique a powerful tool for investigating polar liquids that exhibit much varying reorientation times.

The samples were mixtures of TMU (1,1,3,3-tetramethylurea, >99% purity, used as purchased from Sigma Aldrich) and Millipore grade water. For the concentration dependent studies, mixtures were prepared with different ratios of TMU molecules per water molecules, expressed in terms of $w = ([TMU])/([H_2O])$. The studied concentrations were $w = 0.005$, 0.009, 0.018, 0.036, 0.07, 0.18, 0.25, 0.5, 1, 3, and pure TMU ($w \rightarrow \infty$). For studying the temperature dependence, a mixture with $w = 0.07$, corresponding to a molality of 4 mol/kg or a molarity of 2.7 mol/L at room temperature, was used.

The complex permittivity of the mixtures was determined between 200 MHz and 50 GHz using a frequency-domain reflectometer based on an Agilent 85070E dielectric probe kit, connected to an Agilent E8364B vector network analyzer (VNA) in conjunction with an electronic calibration module (Agilent N4693B).[22] The VNA was operated in one-port reflection mode and was used to determine the complex reflection coefficient, which after analysis using Agilent software yielded the dielectric spectrum of the sample. For all measurements, a calibration was done with an air sample and a mercury sample representing a short circuit. Further calibrations were done following ref 23 with three appropriate liquids with known dielectric properties from the set of H_2O, *N*,*N*-dimethylacetamide,[24] propylene carbonate,[25] benzonitrile,[25] and 1-butanol.[26] All liquids were used as purchased from Sigma Aldrich. The temperature of the sample was controlled with a thermostat to an accuracy of ±0.05 °C. For the frequency range between 60 and 89 GHz, a double-beam interferometer with variable path-length transmission sample cells was used.[27]

For the frequency region between 0.4 and 1.2 THz, a time-domain spectrometer was used. This THz setup was based on terahertz generation in a ZnTe (110) nonlinear crystal, using 800 nm pulses with a duration of ∼150 fs from a Ti-Sapphire laser. The time-dependent electric field strength was measured using the electro-optic effect in a second ZnTe crystal with a variably delayed pulse of 800 nm with a duration of ∼150 fs. A frequency domain analysis of the THz pulse, with a duration of ∼1 ps, transmitted through an empty cell (Infrasil quartz, path length 103 ± 0.5 μm) and the THz pulse transmitted through a filled sample cell yielded the complex frequency-dependent permittivity of the sample. This was done through an analysis where the (multiple) reflection and transmission coefficients for all transitions (air−quartz−sample−quartz−air) were taken into account.[28] A mechanical device was used to position a mixture sample and a pure water sample

(21) Stirnemann, G.; Hynes, J. T.; Laage, D. *J. Phys. Chem. B* **2010**, *114*, 3052–3059.
(22) Hunger, J. Ph.D. thesis, Regensburg, 2010.
(23) Schrödle, S.; Hefter, G.; Kunz, W.; Buchner, R. *Langmuir* **2006**, *22*, 924–932.
(24) Barthel, J.; Buchner, R.; Wurm, B. *J. Mol. Liq.* **2002**, *98−99*, 51–69.
(25) Barthel, J.; Buchner, R.; Hölzl, C. G.; Münsterer, M. *Z. Phys. Chem. (München)* **2000**, *214*, 1213–1231.
(26) Pickl, J. L. Ph.D. thesis, Regensburg, 1998.
(27) Barthel, J.; Bachhuber, K.; Buchner, R.; Hetzenauer, H.; Kleebauer, M. *Ber. Bunsen-Ges. Phys. Chem.* **1991**, *95*, 853–859.
(28) Knoesel, E.; Bonn, M.; Shan, J.; Wang, F.; Heinz, T. *J. Chem. Phys.* **2004**, *121*, 394–404.

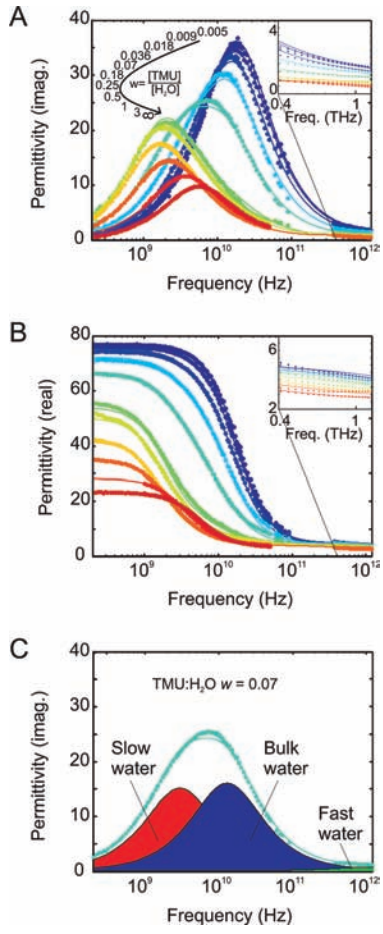

Figure 1. Combined data (dots) and fits (lines) from GHz and THz dielectric relaxation spectroscopy, showing the imaginary (ε'') (A) and real (ε') (B) permittivity as a function of frequency for different TMU concentrations, given in ratios of TMU:H_2O. The insets show the frequency dependence in the THz regime more closely. (C) A decomposition into the three dielectric relaxation processes (slow hydration shell water, bulk-like water and fast water) for $w = 0.07$.

alternatingly in the focus of the THz beam (4 s cycle time).[29] The measurement of pure water with known dielectric properties was then used to calibrate the dielectric properties of the mixture that was measured in parallel. The temperature-dependent measurements were done using a sample cell with a variable optical path length, equipped with a Peltier element, as in ref 30.

Results and Discussion

Concentration Dependence. Data and Fit Results. The results of the combined GHz−THz dielectric relaxation measurements are shown in Figure 1 for a wide range of TMU−water mixtures, measured at 25 °C. First, it is interesting to note that upon increasing the concentration of TMU, the peak of the imaginary permittivity (Figure 1A) first shifts to lower frequencies (corresponding to slower reorientation) and then back to higher frequencies upon further increasing the concentration. It is also clear that the imaginary permittivity has a rather asymmetric shape at those concentrations where the reorientation is slowest. For pure water, two relaxation processes are needed to describe

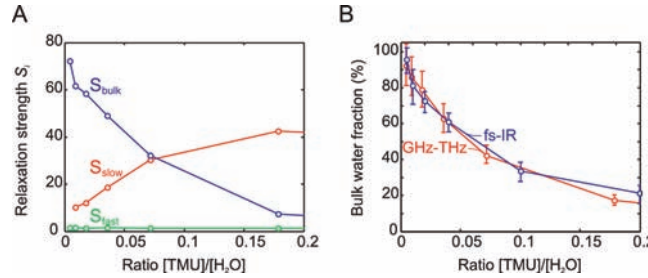

Figure 2. (A) The extracted relaxation strengths S_i for the slow component, the bulk-like water, and the fast water. (B) The extracted fraction of bulk-like water, based on the fits to the GHz−THz data and the fs-IR data, as a function of TMU concentration.

the complex permittivity up to ~1 THz.[31,32] It is apparent from the highly asymmetric signal at intermediate concentrations (e.g., for $w = 0.07$) that the addition of TMU introduces a third, slower Debye relaxation process. Thus, we used the following equation to describe all frequency-dependent permittivities $\hat{\varepsilon}(\omega)$:

$$\hat{\varepsilon}(\omega) = \frac{S_{\text{slow}}}{1 + i\omega\tau_{\text{slow}}} + \frac{S_{\text{bulk}}}{1 + i\omega\tau_{\text{bulk}}} + \frac{S_{\text{fast}}}{1 + i\omega\tau_{\text{fast}}} + \varepsilon_\infty \quad (2)$$

Here, the first term describes the reorientation of the slow component, with a strength S_{slow} and a time scale τ_{slow}. This slow component contains both contributions from slowly reorienting water molecules and from the reorientation of the solute TMU molecules. The second term describes the reorientation of bulk-like water with a strength S_{bulk} and a time scale τ_{bulk}. Finally, the third term describes a fast dipolar reorientation process that has been attributed to undercoordinated water molecules[33] with a strength S_{fast} and a time scale τ_{fast}. The remaining high frequency limit permittivity is given by ε_∞. The high frequency limit is where the transition occurs from the region where relaxation processes are active to the region where resonant processes are active, such as intermolecular hydrogen -bond stretching, located at 5.4 THz,[31,33] and intramolecular OH-stretching, located at 100 THz (3400 cm^{-1}). The strengths S_i are indicative of the dipole density, that is, reflect the number of water molecules that participate in the corresponding Debye processes.

In fitting the data to eq 2, it was assumed that the relative error in the permittivity was constant over the whole frequency range. The results of the fits are shown as lines in Figure 1, where the three relaxation strengths S_i and time scales τ_i are not constrained. Clearly, eq 2 describes the data very well, over nearly four decades of frequencies and more than two decades of concentrations. The fit results for the strengths S_i are shown in Figure 2A; the fit results for the reorientation time scales of the bulk-like water (τ_{bulk}) and slow component (τ_{slow}) are shown in Figure 3, along with the viscosity data from ref 34.

The fit results for the relaxation strengths $S_{\text{slow}} = \varepsilon_S - \varepsilon_1$, $S_{\text{bulk}} = \varepsilon_1 - \varepsilon_2$, and $S_{\text{fast}} = \varepsilon_2 - \varepsilon_\infty$ were used to extract the fractions of the three components. Because the slow mode contains contributions from water dipoles and TMU dipoles,

(29) Tielrooij, K. J.; Timmer, R. L. A.; Bakker, H. J.; Bonn, M. *Phys. Rev. Lett.* **2009**, *102*, 198303.
(30) Tielrooij, K. J.; Paparo, D.; Piatkowski, L.; Bakker, H. J.; Bonn, M. *Biophys. J.* **2009**, *97*, 2484–2492.
(31) Fukasawa, T.; Sato, T.; Watanabe, J.; Hama, Y.; Kunz, W.; Buchner, R. *Phys. Rev. Lett.* **2005**, *95*, 197802.
(32) Rønne, C.; Keiding, S. R. *J. Mol. Liq.* **2002**, *101*, 199–218.
(33) Yada, H.; Nagai, M.; Tanaka, K. *Chem. Phys. Lett.* **2008**, *464*, 166–170.
(34) Okpala, C.; Guiseppi-Elie, A.; Maharajh, D. M. *J. Chem. Eng. Data* **1980**, *25*, 384–386.

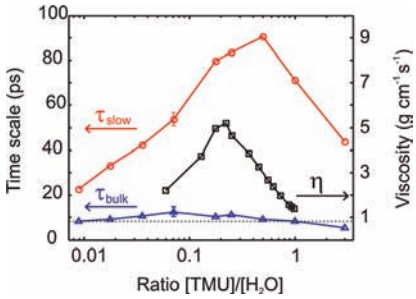

Figure 3. The extracted reorientation time scale for the slow hydration shell water $\tau_{slow}(c)$ (○), the reorientation time scale for bulk-like water $\tau_{bulk}(c)$ (△), and the viscosity (□; data from ref 34) as a function of TMU concentration. The dashed line represents the reorientation time for bulk water $\tau_{bulk}(0)$. Error bars are given as an indication.

we determine the fraction of bulk-like and fast water. For the large range of concentrations studied, it was most appropriate to use the following equation, based on the solvent-normalized Cavell equation,[16,35] to extract the fraction of bulk-like water, as a function of TMU concentration c:

$$f_{bulk}(c) = \frac{[S_{bulk}](c)}{[S_{bulk} + S_{fast}](0)} \frac{c_{H_2O}(0)}{c_{H_2O}(c)} \frac{\tau_{bulk}(0)}{\tau_{bulk}(c)} \frac{(2\varepsilon_S(c) + 1)\varepsilon_S(0)}{\varepsilon_S(c)(2\varepsilon_S(0) + 1)} \quad (3)$$

where $c_{H_2O}(c)$ is the concentration (in mol/L) of water in a TMU−water mixture of concentration c (also in mol/L). In this equation, it is assumed that the effective dipole moment of water in these solutions is the same as in neat water. We take into account the effects of dilution (second factor), dipole−dipole correlations (third factor), and local field effects (fourth factor). For the fraction of fast water, we replace S_{bulk} in the numerator by S_{fast} and remove the dipole−dipole correlation term $(\tau_{bulk}(0))/(\tau_{bulk}(c))$.

Interpretation. The relaxation strengths of the three components show a clear dependence on the concentration (see Figure 2A). The fraction of water with fast dynamics (the process with time scale τ_{fast}) showed an increase from 2% at $w = 0$ to 13% at $w = 1$. This is related to an undercoordination of the water network and is consistent with the observation that the linear absorption spectrum of the OD-stretch vibration shifts to higher frequencies for higher concentrations of TMU in TMU−water mixtures (where the water contained a small fraction of D_2O).[17] This blueshift indicates an overall weakening of the hydrogen-bond network, as concluded previously from isotope-substituted neutron diffraction of a small hydrophobe in water[7] and from theoretical calculations.[36,37] Furthermore, a similar observation of an increased fraction of undercoordinated water was made for weakly hydrated amphiphilic lipid molecules, using THz DR spectroscopy.[30]

The fraction of water with the bulk-like time scale τ_{bulk} decreases with increasing concentration of TMU, as illustrated in Figure 2, while simultaneously the relaxation strength of the slow component increases. The fraction of water that is associated with the bulk-like time scale indeed behaves very much like bulk water: there is very little dependence of the time constant on concentration. For increasing TMU concentrations, the time scale increases somewhat (less than a factor 1.5) and then decreases again (Figure 3). Hence, it appears that these water molecules are surrounded by other water molecules and behave bulk-like at all concentrations.

The slow component contains contributions from both TMU and water dipoles. The relative contributions of TMU and water to the slow component depend on the concentration and are readily calculated from the relaxation strength of the slow component, as compared to the relaxation strength of pure TMU. For instance, for $w = 0.02$, the slow component amounts to ∼17% of the total response of which ∼3% is due to TMU and ∼14% due to water. For $w = 0.2$, the slow component constitutes ∼85% of the total response of which ∼25% is due to TMU and ∼60% due to water. Therefore, for $w < 0.2$, the slow component is dominated by slowly reorienting water molecules that hydrate TMU.

At low concentrations, the fraction of slow water increases linearly with concentration, but starts to show a saturation behavior at $w > 0.07$,[38] in agreement with NMR results.[10,40] The fraction of water that exhibits slower reorientation dynamics is significantly slower at all concentrations. At very low concentrations (<0.1 M), the slowdown factor is ∼3, in good agreement with an earlier DR study.[15] At a moderate concentration of $w = 0.018$ (1 mol/kg), the reorientation dynamics of the slow water fraction is 4 times slower than that of bulk water. This indicates that for these mixtures, there is a significant retardation effect of the reorientation dynamics of water hydrating TMU. The observed time scales also agree with the results of classical molecular dynamics simulations by Wei et al., who found the first-order time correlation function for a 5 mol/L TMU−water solution to be still nonzero after 50 ps,[4] but are significantly longer than was calculated in the classical MD simulations by Laage and Hynes.[3]

The longest reorientation time is found for a TMU−water mixture with about two water molecules per TMU molecule ($w = 0.5$). This time scale (∼90 ps) is more than 10 times longer than the reorientation time of bulk water. For these mixtures, the reorientation of TMU and its hydration shell is also much slower than the reorientation of TMU molecules in pure TMU. This suggests that the small water molecules and the larger TMU molecules together form a dense jammed system. The concentration dependence of the reorientation time correlates very well with the concentration dependence of the viscosity.[34] The viscosity also shows a maximum at a ratio where there are only a few water molecules per TMU, as illustrated in Figure 3. For

(35) Buchner, R.; Chen, T.; Hefter, G. *J. Phys. Chem. B* **2004**, *108*, 2365–2375.
(36) Mancera, R. L. *J. Chem. Soc., Faraday Trans.* **1998**, *94*, 3549–3559.
(37) Graziano, G.; Lee, B. *J. Phys. Chem. B* **2005**, 8103–8107.

(38) This shows that the effect of aggregation is weak and does not strongly affect the observed hydration shell water dynamics. This is in agreement with small-angle X-ray scattering measurements, from which it was concluded that solute aggregation in aqueous TMU solutions is weak.[39]

(39) Almasy, L.; Len, A.; Szekely, N. K.; Plestil, J. *J. Fluid Phase Equilib.* **2007**, *257*, 114–119.

(40) The precise fractions of hydration shell water obtained from NMR and DR cannot be compared directly, because from NMR measurements, one obtains the time-integrated reorientation time constant averaged over the whole solution. Hence, to arrive at a fraction of hydration shell water and an associated reorientation time constant, a certain value for the number of slowed water molecules has to be assumed. Usually, this number is taken equal to the geometric hydration number, which leads to a typical slowing of the hydration shell by a factor of ∼1.5 at room temperature. In the present study, we find that the number of slowed water molecules is significantly (2−3 times) smaller than that contained in the geometric hydration shell. If the NMR measurements would be analyzed using the 2−3 times smaller number of slowed water molecules observed here, a slowing factor of 3−5 would result, which agrees with the present results.

$w = 0.25$, the viscosity is ~5 times higher than for pure water and for pure TMU.

The strong effect of TMU on the dynamics of water even at low concentrations shows that this osmolyte has a strong hydrophobic hydration effect. Hence, it is to be expected that the hydrophobic groups of TMU also favorably interact with the hydrophobic groups of proteins, which could explain why TMU is very effective in stimulating the denaturation of proteins.

Comparison with fs-IR Data. The GHz−THz DR data can be compared to the results from polarization-resolved femtosecond infrared pump−probe studies of the reorientation dynamics in TMU−water mixtures by Rezus et al.,[17] where it was found that a significant fraction of water was present with slower reorientation dynamics. This fs-IR technique studies directly the reorientation dynamics of individual water molecules with high temporal resolution (~150 fs). In these experiments, the OD-stretch vibration of a subset of HDO molecules in H_2O (4% D_2O in H_2O) was excited by a resonant infrared pump pulse with a frequency of ~75 THz (2500 cm^{-1}). Molecules with their OD-group preferentially aligned along the polarization axis of this infrared pump pulse were most efficiently tagged. With a variable time delay, the system was then interrogated by a probe pulse, which measured the number of tagged molecules parallel and perpendicular to the excitation axis. An appropriate ratio of the two signals divides out the effects of vibrational relaxation and provides the anisotropy parameter $R(t)$, which (corrected for heating due to the excitation according to ref 41) as a function of pump−probe delay time t then reflects the orientational dynamics of the probed water molecules. This technique makes it possible to directly monitor the water dynamics during a time window of ~10 ps. Because the limited time window, fs-IR studies[17,18] concluded that the slow hydration shell water is associated with a reorientation time of $\tau_{slow} > 10$ ps.

GHz−THz dielectric relaxation measurements and fs-IR pump−probe spectroscopy are sensitive to the same reorientation processes of water molecules. However, there are four main differences between the two techniques, which are fortunately well understood. (i) GHz−THz dielectric relaxation measurements are sensitive to the inverse Fourier transform of the time derivative of the first-order time correlation function, whereas fs-IR measurements are sensitive to the decay of the second-order time correlation function.[42−44] Because of this difference, the reorientation time found with fs-IR is ~2.5 times shorter than the reorientation time scale found with DR, assuming jump reorientation of water molecules.[45] (ii) GHz−THz dielectric relaxation measurements probe the dynamics of the macroscopic polarization of the sample, while fs-IR measurements probe the dynamics of isolated water molecules. As a result, dielectric relaxation measurements can contain contributions due to local fields and dipole−dipole correlations.[42−44] Because of the local field effects and dipole−dipole correlations, the total difference between the two reorientation times amounts to a factor of ~3.4 for neat water, as experimentally found in ref 42. Furthermore,

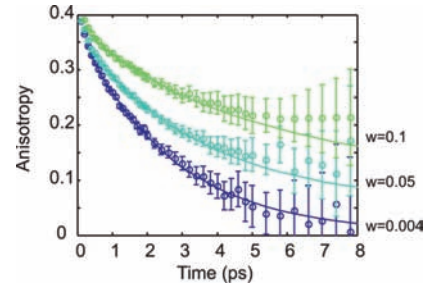

Figure 4. The anisotropy decay as a function of pump−probe delay time for a number of TMU concentrations, from ref 17. To describe these data (lines), the resulting time scales from the GHz−THz measurements $\tau_{slow}(c)$ and $\tau_{bulk}(0)$ were used, after correction for the difference between macroscopic first order (GHz−THz) and microscopic second order (fs-IR) correlation function measurements.

(iii) the two techniques are sensitive to the reorientation of different axes of the molecule: the dipole vector in the case of GHz−THz DR and the OH-vector in the case of fs-IR.[46] If water molecules would reorient in an anisotropic fashion, that is, in preferred directions, this could also result in different reorientation time scales for the two techniques. Finally, (iv) GHz−THz measurements not only probe the orientational dynamics of water dipoles, but also of the solute TMU molecules. Hence, the comparison can be made up to $w = 0.2$, as in this concentration range the slow component is dominated by water molecules hydrating TMU.

To determine if the GHz−THz DR results are in agreement with the data from previous fs-IR measurements, we use the slow reorientation time scales as found from the GHz−THz DR measurements (corrected by a factor of $\zeta \approx 3.4$)[42,47] to describe the fs-IR anisotropy decays:

$$R(t) = A_{bulk} \cdot e^{-\zeta \cdot t/\tau_{bulk}(0)} + A_{slow} \cdot e^{-\zeta \cdot t/\tau_{slow}} \quad (4)$$

Here, $(A_{bulk})/(A_{bulk} + A_{slow})$ and $(A_{slow})/(A_{bulk} + A_{slow})$ represent the fraction of water molecules that exhibit bulk-like dynamics and the fraction of water that has slow dynamics, respectively. In Figure 4, the data from ref 17 are shown, together with biexponential fits based on eq 4. Only the amplitudes A_{bulk} and A_{slow} are adjustable parameters, because the bulk-like reorientation time $\tau_{bulk}(0)$ is fixed to the one for neat water and the slow reorientation time is inferred from the GHz−THz DR measurements. The fast water process (with time scale τ_{fast}, see eq 2) that is present in the GHz−THz DR data does not show up in the fs-IR studies.

The fits in Figure 4 show that the time constants obtained from DR yield a good description of the fs-IR results. Therefore, the corresponding fractions of bulk-like and slow water can also be compared. The results for the bulk-like fractions from GHz−THz DR and fs-IR spectroscopy as a function of TMU concentration are shown in Figure 2B. This figure shows that the results of the two techniques are consistent not only in terms of the inferred reorientation time scales, but also in terms of the fractions of bulk-like water, over a large range of concentrations. The quantitative agreement between the results of the

(41) Rezus, Y. L. A.; Bakker, H. J. *J. Chem. Phys.* **2005**, *123*, 114502.
(42) Tielrooij, K. J.; Petersen, C.; Rezus, Y. L. A.; Bakker, H. J. *Chem. Phys. Lett.* **2009**, *471*, 71–74.
(43) Böttcher, C. J. F. *Theory of Electric Polarization*; Elsevier: Amsterdam, 1973; Vol. I.
(44) Böttcher, C. J. F. *Theory of Electric Polarization*; Elsevier: Amsterdam, 1978; Vol. II.
(45) Laage, D.; Hynes, J. T. *Science* **2006**, *311*, 832–835.
(46) Tielrooij, K. J.; Garcia-Araez, N.; Bonn, M.; Bakker, H. J. *Science* **2010**, *328*, 1006–1009.
(47) Assuming that the conversion factor ζ mainly comes from local field effects, we calculate[44] that ζ decreases by less than 5% at very high TMU concentrations. This validates the assumption of a concentration-independent conversion factor.

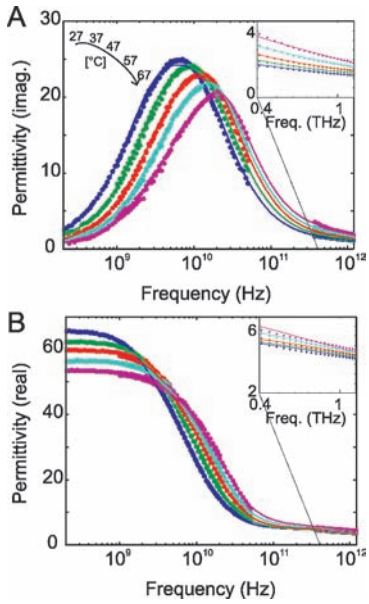

Figure 5. The imaginary (A) and real (B) parts of the permittivity for a solution of TMU in water (4 mol/kg) at different temperatures. The insets show the frequency dependence in the THz regime more closely.

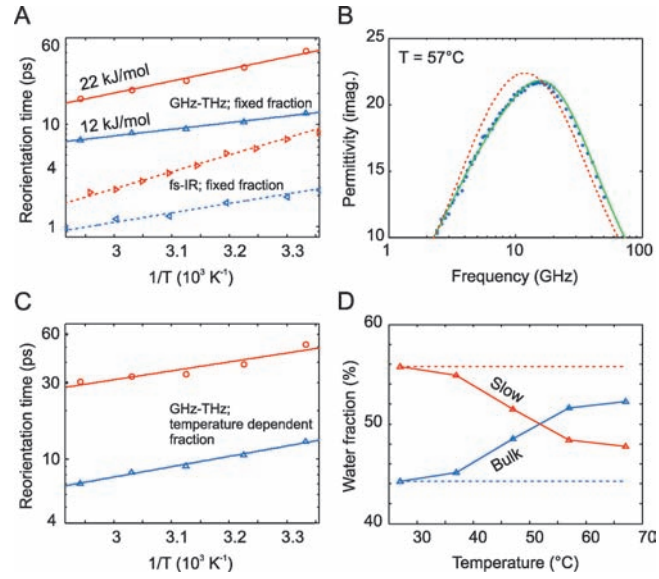

Figure 6. (A) The fit results when the fractions of bulk-like and slow water are fixed for the GHz−THz measurements (○, △), together with fs-IR measurements (right-pointing triangle, left-pointing triangle) from ref 20, where the same assumption was made. (B) A comparison of the fit for TMU $w = 0.07$ at 57 °C, where the fraction of bulk-like is free (line) and where it is kept constant over temperature (dotted line). (C) The reorientation time for bulk-like water (○) and TMU/slow water (△) as a function of $1/T$ with fits where the water fractions were free. Note that the slope of the slow water species in this case does not represent the activation energy of the hydrophobic hydration shell water, as the number of water molecules in this ensemble is not constant with temperature. (D) The fraction of bulk-like water as function of temperature (△) and the fixed fraction of bulk-like water for the alternative fit (dotted line).

GHz−THz DR and fs-IR spectroscopies confirms that the reorientation dynamics of water in solutions of TMU can be described in terms of two major subensembles, bulk-like water and slow water hydrating TMU.

The fractions of bulk-like water as extracted from GHz−THz DR and fs-IR measurements agree well for the whole concentration range (Figure 2B). In the low concentration regime (up to $w = 0.07$), the fraction of bulk water indicates that each TMU molecule slows the dynamics of about 8−12 water molecules, corresponding to 2−3 water molecules per methyl group. This agrees well with fs-IR studies on mixtures of TMU:water and water with other methyl-group containing amphiphiles, where 2 slow water molecules (4 OH-groups) were found per methyl group.[17,18] Previous NMR and fs-IR studies showed that the effect of hydrophobic solutes on the reorientation scales quite well with the number of methyl groups contained in the solute.[10,13,18] Hence, the water network appears to fold around the individual methyl groups, rather than interacting with the hydrophobic part of TMU as if it were a single extended hydrophobic surface. We also find that the number of slowed water molecules is significantly smaller than the number of water molecules contained in the geometric hydration shell. This result can be rationalized by the notion that the water molecules contained in the geometric hydration shell show a strong variation in positions and orientations. Some of the water molecules within the shell can thus experience hydrogen-bond and reorientation dynamics as in bulk water, while for a selected part, these dynamics are strongly slowed.

The time scale of ∼10 ps of the hydrophobic hydration shell is in excellent agreement with the time scale found for TMU:water solutions of 1.5 mol/kg at room temperature.[20] However, this time scale is now found to be dependent on concentration, varying from ∼10 ps at 1 mol/kg to ∼25 ps at higher concentrations (second-order time scales).

Temperature Dependence. In Figure 5, the GHz−THz dielectric spectra are shown for a TMU−water mixture with $w = 0.07$ (4 mol/kg). As in bulk water,[48] at higher temperatures the frequency-integrated permittivity decreases due to a decrease in dipole density and increased thermal fluctuations of the dipoles. However, at THz frequencies the imaginary part of the permittivity increases because the dielectric response extends to higher frequencies as a result of faster reorientation at elevated temperatures. To quantify the behavior of the mixture, the data were fit with eq 2 (see lines in Figure 5). In the fitting procedure, like in the previous section, error weighing was used, based on a constant relative error in the permittivity. Equation 2 is clearly capable of fitting the data very well for all temperatures. We can determine the activation energy of the reorientation of the hydration shell if we assume that for all water molecules in the hydration shell the reorientation becomes equally accelerated by an increase in temperature. Under this assumption, we obtain the reorientation times as shown in Figure 6A. In this figure, we also show Arrhenius fits (connected lines) to the extracted time scales. According to Arrhenius' law $\tau \propto e^{E_{act}/k_B T}$, where E_{act} is the activation energy, in this case of the reorientation, and k_B is Boltzmann's constant. The extracted activation energies are $E_{act}^{bulk} = 12$ kJ/mol, for the bulk-like water fraction, and $E_{act}^{slow} = 22$ kJ/mol for the water in the hydration shell. The activation energy of the bulk-like water fraction is in excellent agreement with the activation energy of pure water from the THz reflection study of ref 49.

The temperature-dependent data from our GHz−THz DR measurements are compared to the fs-IR study by Petersen et

(48) Buchner, R.; Barthel, J.; Stauber, J. *Chem. Phys. Lett.* **1999**, *306*, 57–63.
(49) Rønne, C.; Thrane, L.; Astrand, P. O.; Wallqvist, A.; Mikkelsen, K. V.; Keiding, S. R. *J. Chem. Phys.* **1997**, *107*, 5319–5331.

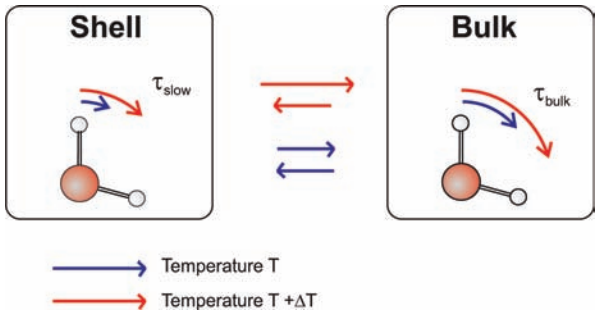

Figure 7. Graphical representation describing the chemical equilibrium between bulk-like water and hydration shell water as a function of temperature, as well as the temperature dependence of the reorientation time. The lower temperature is described by blue arrows; the higher temperature is indicated by red arrows.

al.[20] In this study, 1.5 mol/kg solutions of TMU and tertiary butyl alcohol were studied. It was found that both hydrophobic molecules are surrounded by a hydration shell water with slower dynamics. It was furthermore observed that the relative speedup of the reorientation with temperature was larger for slow hydration shell water than for bulk-like water. An Arrhenius fit showed that the overall activation energy of the slow water fraction was almost twice as large as the overall activation energy of the bulk-like water fraction.[20] Similar observations were done in NMR studies.[11,12] Hence, the present results of our GHz−THz measurements are in excellent agreement with the results of these previous studies.

In Figure 6B, we show the result of the fit for the GHz dielectric spectrum at 57 °C. Clearly, the fit is not optimal: the measured spectrum is much more asymmetric than the fit result. A much better fit can be obtained by allowing the bulk-like water fraction and the slow fraction to change with temperature. The resulting curve fits the GHz spectrum quite accurately. In Figure 6C, the time scales of the reorientation processes of the two subensembles using this approach are given as a function of temperature. In Figure 6D, the corresponding bulk-like and slow fractions are presented. With increasing temperature, the bulk-like water fraction increases while the slow water fraction decreases. Hence, we find that the speedup of the reorientation of the water molecules hydrating TMU is the result of two effects: (i) the transfer of water molecules with hydration shell character to bulk-like character; and (ii) the speedup of the reorientation of water molecules that keep their hydration-shell character. The DR technique allows us to make a distinction between these two contributions. The two contributions are schematically illustrated in Figure 7.

Figure 6C shows that for the water molecules that keep their hydration shell character, the speedup of the reorientation with temperature is the same as for bulk water. This indicates that the reorientation mechanism of water molecules in the shell is probably not very different from that of water molecules in the bulk liquid. It has been proposed that in bulk liquid water the reorientation of an OH group proceeds through a transient bifurcated hydrogen-bond configuration.[45] The much slower reorientation of water in the hydration shell thus suggests that the rate at which the hydrogen-bond structure evolves to a bifurcated state is much lower in the hydration shell than in the bulk liquid.

The transition of water molecules from hydration-shell character to bulk-like character suggests that the size of the hydrophobic hydration shell decreases with temperature. Of course, the water molecules will not significantly change their position in the solution upon a temperature increase. Therefore, the transition to bulk-like character implies that the range over which the hydrophobic molecular groups affect the water hydrogen-bond network decreases. Because the hydrophobe is surrounded by the same geometrical hydration shell at all temperatures, this points to a decrease in the correlation length of the hydrogen-bond network around hydrophobic surfaces. At higher temperatures, the hydrogen-bond network is more dynamic and less coordinated, and therefore the effect of the hydrophobic group will have a shorter persistence length. The effect of a smaller effective hydration shell at higher temperatures is thus also connected with more pronounced interfacial density fluctuations[50] and is consistent with the increases of excess entropy and enthalpy changes of the hydrophobic hydration.[51]

The decrease of the hydrophobic hydration shell with temperature shows that the retardation effect on the reorientation is not a simple excluded volume effect, as recent computer simulations have suggested.[3] The excluded volume is a purely geometrical effect: the reorientation of water molecules adjacent to a hydrophobe experiences an excluded volume, where no new hydrogen bond partners can be found, leading to slower reorientation. When the temperature is changed, the molar volumes of water and TMU stay more or less constant,[52] meaning that the geometry of the system is unaltered. Hence, the fraction of slow hydration shell water would not be expected to change with temperature, based on the excluded volume effect. The observation that there is a change in the fraction of slow hydration shell water with temperature shows that other effects play a role, in addition to the excluded volume effect.

Conclusions

By measuring the GHz−THz dielectric response in TMU−water mixtures over a range of concentrations and for different temperatures, a better molecular level understanding of hydrophobic hydration has been obtained. We find that there is a substantial retardation of the dynamics of water directly surrounding the hydrophobe, where the reorientation dynamics are between 3 (at low concentrations) and 10 (at higher concentrations) times slower than the dynamics of bulk water. It is furthermore clear that the effect of the hydrophobe is relatively short-ranged: the dynamics of 8−12 (at concentrations below $w = 0.07$) water molecules per TMU molecule show substantial retardation; the other water molecules behave bulk-like.

By changing the temperature for a TMU:water mixture with about 14 water molecules per TMU molecule ($w = 0.07$), it was shown that the overall activation energy of the slow hydration shell water is about twice as large as for bulk water. Because the GHz−THz measurements can separately determine the reorientation time scales and fractions of slow and bulk-like water, it was found that the fraction of bulk-like water increases with increasing temperature, thus explaining

(50) Mittal, J.; Hummer, G. *Proc. Natl. Acad. Sci. U.S.A.* **2008**, *105*, 20130–20135.
(51) Southall, N. T.; Dill, K. A.; Haymet, A. D. J. *J. Phys. Chem. B* **2002**, *106*, 521–533.
(52) The density of the TMU−water mixture with $w = 0.07$ has been measured with a vibrating tube densimeter (Anton Paar DMA 60/601 HT) and showed that the density decreased by less than 2% between 25 and 67 °C.

the higher activation energy for hydration shell water. This temperature effect indicates that the hydrophobic interaction decreases with temperature. It furthermore shows that the retardation effect is not the result of a simple excluded volume effect. Instead, the retardation results from a more collective frustration of the structural dynamics of the hydrogen-bond network of water by the hydrophobic molecular groups.

Acknowledgment. This work is part of the research program of the "Stichting voor Fundamenteel Onderzoek der Materie (FOM)", which is financially supported by the "Nederlandse organisatie voor Wetenschappelijk Onderzoek (NWO)". We thank H. Schoenmaker for technical support, and Yves Rezus and Christian Petersen for discussions and providing data.

JA106273W